Synthesis, in Vitro Evaluation and Cocrystal Structure of 4-Oxo-[1]benzopyrano[4,3-c]pyrazole *Cryptosporidium parvum* Inosine 5′-Monophosphate Dehydrogenase (*Cp*IMPDH) Inhibitors

Zhuming Sun,[†] Jihan Khan,[§] Magdalena Makowska-Grzyska,[∥] Minjia Zhang,[‡] Joon Hyung Cho,[†] Chalada Suebsuwong,[†] Pascal Vo,[†] Deviprasad R. Gollapalli,[‡] Youngchang Kim,[∥,⊥] Andrzej Joachimiak,[∥,⊥] Lizbeth Hedstrom,[‡,§] and Gregory D. Cuny*,[†]

[†]Department of Pharmacological and Pharmaceutical Sciences, College of Pharmacy, University of Houston, Science and Research Building 2, Room 549A, Houston, Texas 77204, United States

[‡]Departments of Biology and [§]Chemistry, Brandeis University, 415 South Street, Waltham, Massachusetts 02454, United States

[∥]Center for Structural Genomics of Infectious Diseases, Computational Institute, University of Chicago, 5735 South Ellis Avenue, Chicago, Illinois 60637, United States

[⊥]Structural Biology Center, Biosciences, Argonne National Laboratory, 9700 South Cass Avenue Argonne, Illinois 60439, United States

S *Supporting Information*

ABSTRACT: *Cryptosporidium* inosine 5′-monophosphate dehydrogenase (*Cp*IMPDH) has emerged as a therapeutic target for treating *Cryptosporidium* parasites because it catalyzes a critical step in guanine nucleotide biosynthesis. A 4-oxo-[1]benzopyrano[4,3-*c*]pyrazole derivative was identified as a moderately potent (IC_{50} = 1.5 μM) inhibitor of *Cp*IMPDH. We report a SAR study for this compound series resulting in **8k** (IC_{50} = 20 ± 4 nM). In addition, an X-ray crystal structure of *Cp*IMPDH·IMP·**8k** is also presented.

8k
*Cp*IMPDH IC_{50} = 20 ± 4 nM
*h*IMPDH2 < 20% inhibition at 5 μM
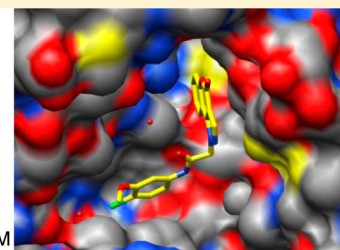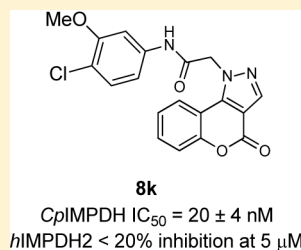
INTRODUCTION

Cryptosporidium parvum and *Cryptosporidium hominis* are intracellular protozoan parasites that invade the brush border epithelial cells of the small intestine. Cryptosporidiosis is prevalent in the developing world where it results in life-threatening diarrhea and severe malnutrition in children.[1]

Cryptosporidium oocysts are water-transmitted and highly resistant to water purification methods, also leading to significant disease burden in the developed world.[2] Infections resolve in immunocompetent hosts but can be chronic and fatal in immunocompromised patients. Furthermore, because oocysts can readily be obtained and water supplies are relatively easily accessed, these organisms represent a credible bioterrorism threat.[3] Currently, vaccine therapies against *C. parvum* and *C. hominis* are not available and the only approved drug, nitazoxanide, has an ill-defined mechanism of action and is not particularly effective.[4] Thus, new chemotherapeutic agents are needed for the treatment of cryptosporidiosis.

One emerging molecular target for the treatment of cryptosporidiosis is the oxidoreductase inosine 5′-monophosphate dehydrogenase (IMPDH), which catalyzes the conversion of inosine-5′-monophosphate (IMP) into xanthosine-5′-monophosphate (XMP) as the rate-determining step in guanine nucleotide biosynthesis.[5] Genomic analysis revealed that *Cryptosporidium* cannot synthesize purine nucleotides de

novo.[6−8] Instead, the parasite converts adenosine salvaged from the host into guanine nucleotides via a linear pathway dependent on IMPDH activity. Interestingly, these parasites appear to have obtained their IMPDH gene by lateral gene transfer from bacteria. Consequently, *Cp*IMPDH is structurally distinct from mammalian IMPDH enzymes[9] and is poorly inhibited by the prototypical human IMPDH inhibitor mycophenolic acid (*Cp*IMPDH IC_{50} ∼ 10 μM; *h*IMPDH1 K_i = 33 nM; *h*IMPDH2 K_i ∼ 7 nM).[10,11] These structural and mechanistic differences also provide an opportunity to design selective *Cp*IMPDH inhibitors as therapeutic agents for treating cryptosporidiosis.[12] *Cp*IMPDH inhibitors may also be effective against bacterial infections.[13,14]

Previously, we have reported the optimization of several structurally distinct compound series, including **C64** and **Q21**,[15−18] as well as the first demonstration of in vivo efficacy of a *Cp*IMPDH inhibitor (e.g., **P131**) in a mouse model of cryptosporidiosis (Figure 1).[19] This later study also revealed several additional hurdles required in the development of efficacious compounds, including preferential compound distribution to gastrointestinal enterocytes (as opposed to systemic distribution) and minimizing the impact of IMPDH
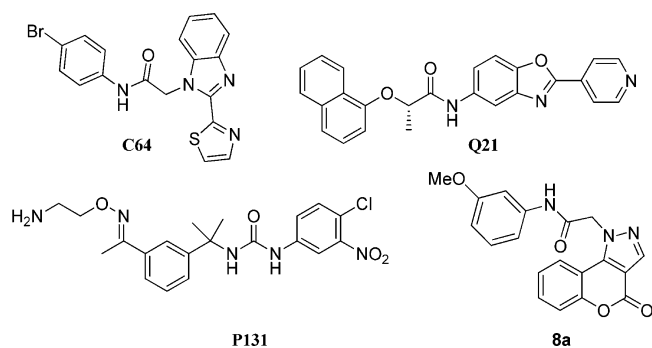
Figure 1. Structures of previously described inhibitors **C64** and **Q21** that have been cocrystallized with *Cp*IMPDH, **P131** that demonstrated in vivo efficacy in a cryptosporidiosis animal model, and a new inhibitor **8a** identified by HTS.

inhibition on gut microbiome populations. The study reported herein is a continuation of our effort to identify and optimize structurally distinct *Cp*IMPDH inhibitors and to develop a common pharmacophore as a guide for the future design of additional *Cp*IMPDH inhibitors.

Our current structure−activity relationship (SAR) study was initiated based on 4-oxo-*N*-(3-methoxyphenyl)-[1]-benzopyrano[4,3-*c*]pyrazole-1(4*H*)-acetamide (**8a**, Figure 1), identified by high throughput screening, as a moderately potent *Cp*IMPDH inhibitor (IC$_{50}$ = 1.5 ± 0.2 μM).

■ RESULTS AND DISCUSSION

Chemistry. 4-Oxo-[1]benzopyrano[4,3-*c*]pyrazole analogues (**8a−n** and **13a−f**) were prepared using four general synthetic methods. The synthesis of analogues **8a−k** used the methodology shown in Scheme 1 (method A). Anilines **2a−k**

**Scheme 1. Synthesis of 4-Oxo-[1]benzopyrano[4,3-*c*]pyrazole Derivatives 8a−k (Method A)^a**
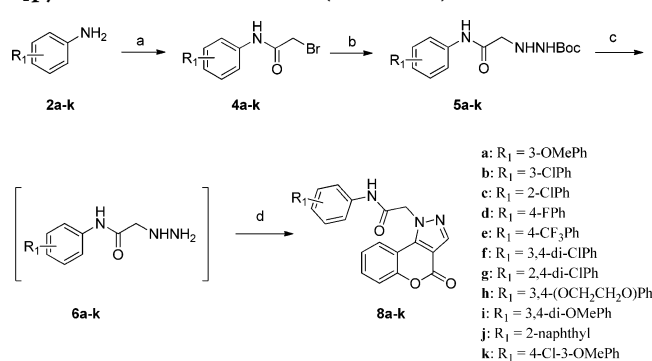
^{a}Reagents and conditions: (a) bromoacetyl chloride (**3**), K$_2$CO$_3$, CH$_2$Cl$_2$, 0 °C to rt; (b) *t*-butyl carbazate, KHCO$_3$, EtOAc/H$_2$O (1:2), 85 °C, 5 h; (c) TFA in CH$_2$Cl$_2$ (1:4), 2 h; (d) 4-chloro-3-formylcoumarin (**7a**), AcOH (cat), EtOH, 105 °C, 20 min.

were treated with bromoacetyl chloride, **3**, in CH$_2$Cl$_2$ in the presence of K$_2$CO$_3$ to afford aryl amides **4a−k**, which were treated with *t*-butyl carbazate in aqueous KHCO$_3$ to provide the *N*-Boc-protected hydrazines **5a−k** via an S$_N$2 reaction. In the next step, trifluoroacetic acid was used to remove the *t*-butyl carbamate protecting group in **5a−k** to give **6a−k**, which were used without purification. The hydrazines **6a−k** were refluxed in ethanol with 4-chloro-3-formylcoumarin (**7a**) in the presence of a catalytic amount of acetic acid to provide analogues **8a−k**.

The presence of the acid proved crucial for these reactions.[20] The regioisomeric [1]benzopyrano[4,3-*c*]pyrazol-4(2*H*)-one derivative **9c** was prepared using the methodology outlined in Scheme 2 (method B). 4-Hydroxycoumarin (**9a**) was treated

Scheme 2. Synthesis of Regioisomers 9c (Method B)^a
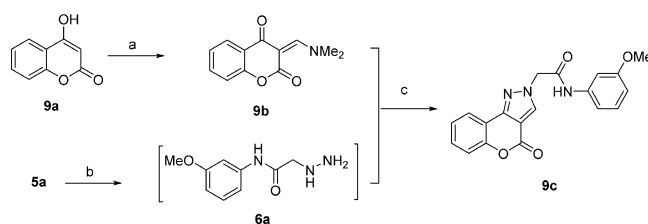
^{a}Reagents and conditions: (a) POCl$_3$, DMF, 1,2-dichloroethane, rt, 12 h, then saturated aqueous Na$_2$CO$_3$; (b) *t*-butyl carbazate, KHCO$_3$, ethyl acetate, 85 °C, 5 h, then TFA in CH$_2$Cl$_2$ (1:4), 2 h, rt; (c) DIPEA, EtOH, rt, 12 h.

with POCl$_3$ and DMF, similar to standard Vilsmeier−Haack conditions, but at room temperature. The reaction was terminated by the addition of aqueous Na$_2$CO$_3$, which generated product **9b**. Upon reaction with **6a** in ethanol in the presence of DIPEA, the regioisomeric pyrazole **9c** was obtained. Presumably, the terminal NH$_2$ of hydrazine **6a** condensed with the carbonyl of the vinylogous amide of **9b**, which was followed by cyclization via an addition−elimination reaction to generate the isolated product.[21]

The preparation of **8l−n**, as analogues of **8k** with additional substituents on the acetamide and [1]benzopyrano[4,3-*c*]-pyrazole, is outlined in Scheme 3 (method C). Anilines **2l** or **2k**

Scheme 3. Synthesis of 4-Oxo-[1]benzopyrano[4,3-*c*]pyrazole Analogue 8l−n (Method C)^a
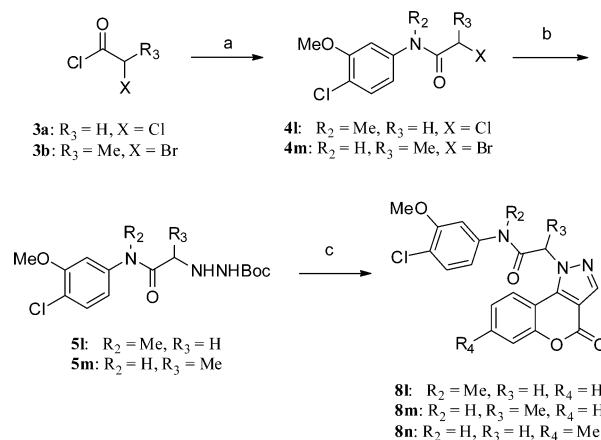
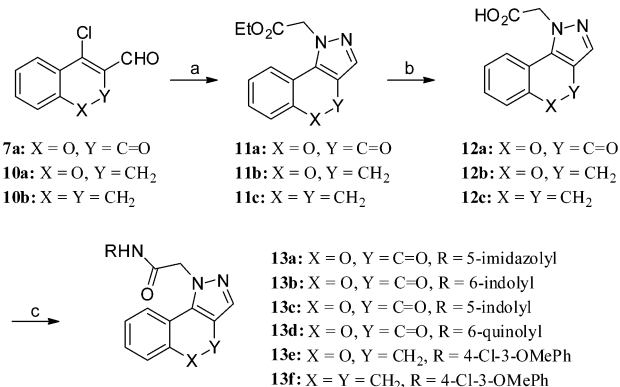

^{a}Reagents and conditions: (a) **2l** (4-Cl-3-OMePhNHMe) or **2k** (4-Cl-3-OMePhNH$_2$), K$_2$CO$_3$, CH$_2$Cl$_2$, 0 °C to rt; (b) for **4l**, *t*-butyl carbazate, K$_2$CO$_3$, KI, acetone, 65 °C, 18 h or for **4m**, *t*-butyl carbazate, DIPEA, toluene 105 °C, 16 h; (c) TFA in CH$_2$Cl$_2$ (1:4), 2 h, then **7a** (or 4-chloro-3-formyl-7-methylcoumarin, **7b**), AcOH (cat.), EtOH, 105 °C, 20 min.

were treated with **3a** or **3b** to afford aryl amides **4l** or **4m**. A stronger base (e.g., K$_2$CO$_3$), organic solvent (e.g., acetone), and the presence of potassium iodide were required to displace the primary chloride of **4l** to furnish **5l**. In the case of **5m**, DIPEA in toluene proved effective. The required intermediate **7b** was synthesized from the corresponding 4-hydroxycoumarin

following typical Vilsmeier−Haack conditions (see Experimental Section). Analogues **8l−n** were synthesized from acid-catalyzed cyclization of hydrazines (**5l−m** des-Boc intermediates) and **7a** or **7b** using the same method described in Scheme 1.

Initial attempts to synthesize analogues **13a−f** following the methodology outlined in Scheme 1 (method A) proved problematic. Thus, an alternate method was developed that is shown in Scheme 4 (method D). Aldehydes **7a** and **10a−b**

Scheme 4. Synthesis of Derivatives 13a−f (Method D)[a]

13a: X = O, Y = C=O, R = 5-imidazolyl
13b: X = O, Y = C=O, R = 6-indolyl
13c: X = O, Y = C=O, R = 5-indolyl
13d: X = O, Y = C=O, R = 6-quinolyl
13e: X = O, Y = CH₂, R = 4-Cl-3-OMePh
13f: X = Y = CH₂, R = 4-Cl-3-OMePh

7a: X = O, Y = C=O
10a: X = O, Y = CH₂
10b: X = Y = CH₂

11a: X = O, Y = C=O
11b: X = O, Y = CH₂
11c: X = Y = CH₂

12a: X = O, Y = C=O
12b: X = O, Y = CH₂
12c: X = Y = CH₂

[a]Reagents and conditions: (a) ethyl hydrazinoacetate hydrochloride (**14**), AcOH (cat), EtOH, 105 °C, 0.5−2 h; (b) **12a**, LiOH (aq), THF, rt, 12 h then EDC, TEA, DMF, **12b−c**, aqueous LiOH, THF, rt, 12 h; (c) NH₂R, HBTU, DIPEA, DMF, rt, 12 h.

were refluxed in the presence of ethyl hydrazinoacetate hydrochloride and a catalytic amount of acetic acid in ethanol to afford pyrazoles **11a−c**. Hydrolysis of the ester using 2 M aqueous LiOH in THF afforded acids **12b−c**. In the case of **12a**, the lactone ring also opened during this step and required relactonization using EDC and TEA in DMF. The acids **12a−c** were treated with either 4-chloro-3-methoxyaniline or heterocyclic anilines in the presence of HBTU and DIPEA in DMF to afford analogues **13a−f**. Intermediates **10a−b** were again prepared using Vilsmeier−Haack reactions (see Experimental Section).

Predicted Binding Mode of Inhibitor 8a with CpIMPDH·IMP. Inhibitor **8a** was docked into the binding site observed in one of our previously reported crystal structures of the catalytic domain of CpIMPDH (PDB code: 4IXH)[15] using AutoDock Tools 1.5.6. The top 10 binding conformations were examined, and the two best conformations (binding energies of −7.86 and −7.76 kcal/mol, respectively) were selected based on similarity of their binding modes with **Q21**,[15] including π-interactions between the 4-oxo-[1]-benzopyrano[4,3-c]pyrazole with the hypoxanthine of IMP and the 3-methoxyphenyl with Y358′ (where prime denotes a residue from the adjacent subunit). However, the hydrogen atom of the amide for these two conformations formed ionic−dipole interactions with two different oxygen atoms in the side chain of E329. Therefore, the conformation that formed an interaction similar to **Q21** was selected as the predicted binding mode for the N-series and is shown in Figure 2.

Evaluation of CpIMPDH Inhibition. Biological characterization of the 4-oxo-[1]benzopyrano[4,3-c]pyrazole derivatives was performed following our published procedures.[15,16] CpIMPDH was expressed and purified as previously reported.[22−24] Enzymatic activity was monitored by NADH
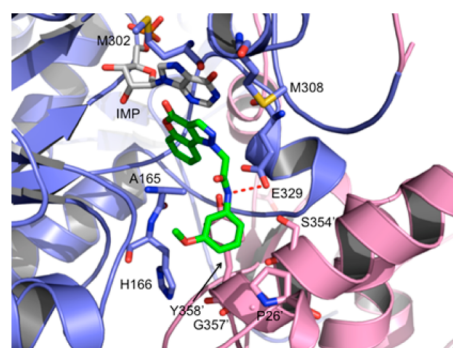
Figure 2. Predicted binding mode of **8a** (green) in complex with CpIMPDH·IMP. The red dotted line indicates an ionic−dipole interaction between the amide of **8a** and the side chain of E329. The phenyl ring of **8a** is stacked above Y358′.

production.[12] IC₅₀ values were determined by averaging the results of three independent experiments unless otherwise noted.

The regioisomeric derivative **9c** did not inhibit CpIMPDH, indicating that the relative orientation of the anilide on the fused pyrazole was crucial for inhibitory activity (Table 1).
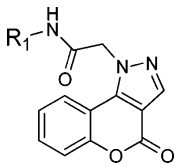
Table 1. Monosubstituted N-Phenyl 4-Oxo-[1]benzo Pyrano[4,3-c]pyrazole-1(4H)-acetamide Derivatives for CpIMPDH Inhibition
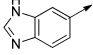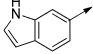

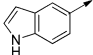| ID	method	R₁	IC₅₀ (nM)
9c	B		>5000
8a	A	3-OMe	1500 ± 200
8b	A	3-Cl	>5000
8c	A	2-Cl	>5000
8d	A	4-F	460 ± 95
8e	A	4-CF₃	580 ± 130

Next, the SAR study focused on the monosubstituted aniline moiety of **8a**. Analogues with a 2-chloro substituent (**8c**) showed no inhibitory activity. Replacement of the 3-methoxy with a chlorine (**8b**) likewise led to loss of inhibition. However, the 4-fluoro and 4-trifluoromethyl derivatives (**8d** and **8e**) displayed a 3-fold increase in activity, indicating that monosubstitution on the amide phenyl moiety could provide only moderate increases in potency, similar to our observation with other inhibitor series.[15,16,18] Therefore, disubstituted and fused anilines were examined. The 2,4-dichloro substituted analogue **8g** showed no inhibition activity (Table 2). In light of this finding, combined with the result of **8c**, it appeared that an ortho-chloro was not well tolerated in the binding pocket, possibly due to a clash with Y358′. However, the 3,4-dichloro analogue **8f** displayed significantly improved potency. A further increase in potency was achieved by replacing the 3-chloro substituent with a methoxy (**8k**, CpIMPDH IC₅₀ = 20 ± 4 nM). However, replacing the remaining chloro of **8k** with another methoxy (**8i**) resulted in the loss of enzyme inhibition. Tethering the ethers into a dioxane ring (**8h**) also resulted in a significantly lower IC₅₀ value compared to **8k**. The loss of activity for these two derivatives containing electron donating

Table 2. Disubstituted *N*-Phenyl and *N*-Heteroaryl 4-Oxo-[1]benzopyrano[4,3-*c*]pyrazole-1(4*H*)-acetamide Derivatives for *Cp*IMPDH Inhibition
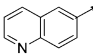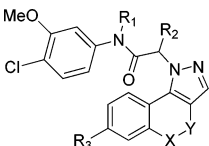

ID	Method	R$_1$	IC$_{50}$ (nM)
8f	A	3,4-di-ClPh	44 ± 7
8g	A	2,4-di-ClPh	> 5000
8h	A	3,4-(OCH$_2$CH$_2$O)Ph	190 ± 30
8i	A	3,4-di-OMePh	2500
8j	A	2-naphthyl	67 ± 35
8k	A	4-Cl-3-OMePh	20 ± 4
13a	D	*(benzimidazol-5-yl)*	2500
13b	D	*(1H-indol-5-yl)*	120 ± 30
13c	D	*(1H-indol-5-yl)*	> 5000
13d	D	*(quinolin-6-yl)*	80 ± 40

groups in the para-position of the anilide is potentially due to weakening of the H-bond donating ability of the amide NH, which is a critical interaction with E329 observed in cocrystal structures of other *Cp*IMPDH inhibitors.[15,25] However, the naphthyl substituted analogue **8j** demonstrated an IC$_{50}$ value of 67 nM.

On the basis of these results, bioisosteres of the naphthyl were investigated. Benzo[*d*]imidazole **13a** and 1*H*-indol-5-yl **13c** had only weak or no inhibitory activity. However, the (1*H*)-indole **13b** and quinolin-6-yl **13d** showed moderate inhibition (*Cp*IMPDH IC$_{50}$ = 120 ± 30 and 80 ± 40 nM, respectively), albeit less than **8j**.

Further modifications were performed on **8k** that retained the 3-methoxy-4-chloro phenyl moiety (Table 3). Addition of a methyl group on the amide nitrogen (**8l**) resulted in loss of activity, again indicating the importance of the H-bond donor function of the amide NH. Addition of a methyl group on the

Table 3. Modifications of the Acetamide and 4-Oxo-[1]benzopyrano[4,3-*c*]pyrazole Regions of 8k for *Cp*IMPDH Inhibition

| ID	method	R$_1$	R$_2$	R$_3$	X	Y	IC$_{50}$ (nM)
8k	A	H	H	H	O	C=O	20 ± 4
8l	C	Me	H	H	O	C=O	>5000
8m	C	H	Me	H	O	C=O	63 ± 11
8n	C	H	H	Me	O	C=O	2000
13e	D	H	H	H	O	CH$_2$	70 ± 27
13f	D	H	H	H	CH$_2$	CH$_2$	100 ± 30

methylene position (**8m**) resulted in a 3-fold loss of potency, likely due to a steric clash with the side chain of E329. The addition of a methyl to the 7-position of the 4-oxo-[1]benzopyrano[4,3-*c*]pyrazole ring system (**8n**) was also detrimental, revealing the steric limitation of this region of the molecule, likely the result of clashes with either M302 or the ribose of IMP. Replacing the lactone ring with an ether bridge (**13e**) resulted in a 3-fold loss of inhibition, indicating the carbonyl contributes to binding. Replacement of the lactone with an ethylene bridge (**13f**) resulted in a further decrease of potency. Therefore, the lactone appears essential for *Cp*IMPDH inhibition, although the rationale for this observation was not obvious from the docking model.

The original screening hit (**8a**) in addition to 11 other *Cp*IMPDH inhibitors (e.g., **8d−f**, **8h**, **8j**, **8k**, **8m**, **13b**, and **13d−f**) failed to inhibit *h*IMPDH2 (<20% inhibition at 5 μM), which also has high sequence identity (85%) to *h*IMPDH1. These results demonstrated that *Cp*IMPDH inhibitory potency could be increased, while preserving selectivity against a human orthologue.

Crystal Structure of *Cp*IMPDH·8k·IMP. The structure of a *Cp*IMPDH complex with IMP and **8k** was solved at 2.40 Å resolution using molecular replacement with the structure of apo *Cp*IMPDH (PDB code: 3FFS)[25] as the search model. Like the structures of *Cp*IMPDH·IMP in complex with other inhibitors,[15,25] the 4-oxo-[1]benzopyrano[4,3-*c*]pyrazole-based inhibitor interacts with residues from two adjacent subunits. One aromatic moiety of **8k**, the 4-oxo[1]benzopyrano[4,3-*c*]pyrazole, π-stacks with the hydroxanthine of IMP (Figure 3A) in an interaction similar to that observed previously for two other *Cp*IMPDH complexes and as predicted in the docking of **8a**.[15,26] The pyrazole portion interacts with the side chain of M308 and forms n−π* contacts between the carbonyl group of the 4-oxo[1]benzopyrano-[4,3-*c*]pyrazole moiety and the main chain carbonyl of M302.[26] This latter interaction was not predicted in the docking model but provides an explanation for the importance of the lactone. The remaining portion of the inhibitor circumvents A165 and extends into the pocket formed at the subunit interface. The amide NH of **8k** forms a H-bond with a side chain oxygen atom of E329 and is part of the extensive H-bonding network involving T221, S354′, and Y358′. Another common feature observed in all *Cp*IMPDH inhibitor complexes is the interaction of the second aromatic moiety of the inhibitor with the side chain of Y358′. In the case of **8k**, this interaction is observed for the 4-chloro-3-methoxyphenyl. In addition, this moiety is involved in contacts with H166 and P26′ via polar and van der Waals interactions. Inhibitor **8k** does not extend as deep into the cavity formed at the subunit interface as does the 2-(4-pyridyl)benzoxazole derivative **Q21** (Figure 3B).[15] However, similarly to the bromo substituent of inhibitor **C64**,[25] the chloro substituent of **8k** is contacting the main chain carbonyl oxygen atom of G357′ (Figure 3C).

■ CONCLUSION

An SAR study of *Cp*IMPDH inhibitor **8a** was conducted with guidance from an in silico docking model based on a previously crystallized *Cp*IMPDH inhibitor complex. The orientation of the anilide on the fused pyrazole was crucial, a 4-chloro-3-methoxy substitution on the anilide (e.g., **8k**) achieved the greatest potency among this series of derivatives, and the secondary amide and the lactone of the 4-oxo-[1]benzopyrano-[4,3-*c*]pyrazole were vital for binding. Overall, this study
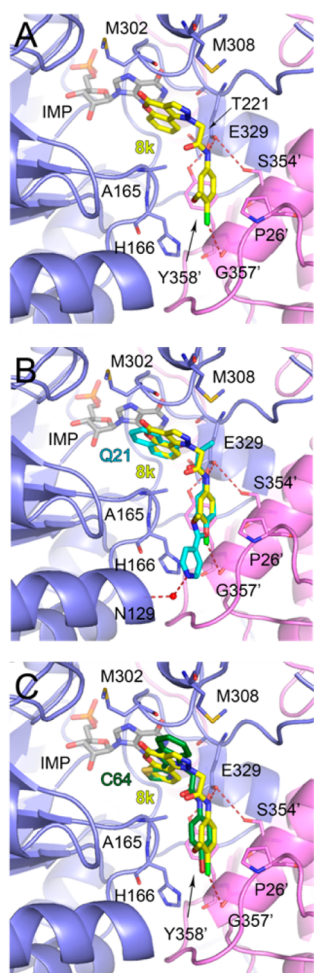
Figure 3. (A) Structure of *Cp*IMPDH·IMP·**8k**. (B) Overlay of *Cp*IMPDH structures with **8k** and **Q21**. (C) Overlay of *Cp*IMPDH structures with **8k** and **C64**. In all panels, chains A (slate) and D (violet) are shown in cartoon representations. Residues involved in IMP and inhibitor binding are shown as sticks. IMP (light gray), **8k** (yellow), **C64** (green), and **Q21** (teal) are shown as sticks. Hydrogen and halogen bonds are depicted as red dashed lines and a water molecule as a red sphere. Prime indicates residues from an adjacent monomer.

provides a structurally distinct inhibitor series that will further assist in the continuing development of *Cp*IMPDH inhibitors for the treatment of cryptosporidiosis and possibly other infectious diseases.[13,14] Finally, a crystal structure of *Cp*IMPDH·IMP and **8k** (e.g., **N109**) provides further support for a general binding mode of *Cp*IMPDH inhibitors featuring three key interactions: (i) π-interaction between an aryl/heteroaryl moiety and the hydroxanthine of IMP, (ii) H-bond with E329, and (iii) extension of an aryl/herteroaryl group into an adjacent subunit forming interactions with Y358′. This pharmacophore provides a template that can be extended to the discovery of other structurally distinct chemical scaffolds of selective *Cp*IMPDH inhibitors.

■ EXPERIMENTAL SECTION

Chemistry. All test compounds had a purity ≥95% as determined by HPLC analyses.

General Procedure for 4a−m. To a suspension of **2a−l** (6.5 mmol) in 15 mL of CH_2Cl_2 at 0 °C, acyl halides (**3** or **3a−b**, 8.5 mmol) and K_2CO_3 (1.25 g, 9.1 mmol) were added. The reaction was maintained at 0 °C for 20 min and then allowed to warm to rt. Saturated aqueous $NaHCO_3$ was added. The reaction mixture was extracted with CH_2Cl_2, and the organic layer was washed by brine, dried over anhydrous Na_2SO_4, filtered, and evaporated in vacuo. The product was purified by column chromatography (0−50% EtOAc in hexane) to afford **4a−m**.

General Procedure for 5a−k. Compound **4a−k** (5.6 mmol), *t*-butyl carbazate (11.2 mmol), and $KHCO_3$ (16.8 mmol) were suspended in 30 mL of EtOAC and H_2O (1:2). The mixture was refluxed at 85 °C for 5 h. The mixture was allowed to cool to rt, and the crude product was extracted with EtOAC, dried with anhydrous $MgSO_4$, filtered, and concentrated. The product was purified by column chromatography (10−70% EtOAc in hexane).

t-Butyl 2-(2-((4-Chloro-3-methoxyphenyl)(methyl)amino)-2-oxoethyl)hydrazinecarboxylate (5l). Compound **4l** (1 mmol), *t*-butyl carbazate (2 mmol), K_2CO_3 (3 mmol), and KI (2 mmol) were suspended in 20 mL of acetone. The mixture was heated at 65 °C for 18 h, allowed to cool to rt, and then evaporated to dryness. The residue was diluted with aqueous NH_4Cl and extracted with EtOAc (20 mL × 3). The organic layer was dried over anhydrous $MgSO_4$, filtered, and concentrated. The product was purified by silica gel column chromatography (5% EtOAc in CH_2Cl_2) to give **5l** as an oil (66% yield).

t-Butyl 2-(1-((4-Chloro-3-methoxyphenyl)amino)-1-oxopropan-2-yl)hydrazinecarboxylate (5m). Compound **4m** (1.7 mmol), *t*-butyl carbazate (3.3 mmol), and DIPEA (3.3 mmol) were suspended in 10 mL of toluene. The mixture was refluxed at 105 °C for 16 h, allowed to cool to rt, and then evaporated to dryness. The residue was diluted with aqueous NH_4Cl and extracted with EtOAc (20 mL × 3). The organic layer was dried over anhydrous $MgSO_4$, filtered, and concentrated. The crude product was purified by silica gel chromatography (0−50% EtOAc in hexane) to give **5m** as a solid (83% yield).

General Procedures for 8a−n. Compounds **5a−m** (0.8 mmol) were treated with 2.5 mL of TFA in CH_2Cl_2 (1:4) at rt for 2 h. The mixture was evaporated in vacuo to afford **6a−m** as colorless oils. The intermediates **6a−m** were dissolved in 2 mL of EtOH, which was then added to a suspension of **7a−b** (0.8 mmol) in 2 mL of EtOH. Acetic acid (20 μL) was added. The mixture was refluxed at 105 °C for 20 min then allowed to cool to rt. The mixture was evaporated in vacuo, partitioned between aqueous $NaHCO_3$ and EtOAc. The organic layer was dried over anhydrous $MgSO_4$, filtered, and concentrated. The products **8a−n** was collected after silica gel chromatography using 20−85% EtOAc in hexane as eluent.

3-[(Dimethylamino)methylene]chroman-2,4-dione (9b). 4-Hydroxycoumarin (**9a**, 9.2 mmol) in 1.5 mL of DMF added to 10 mL of 1,2-dichloroethane. To this solution was added 1.1 mL of $POCl_3$. The mixture was stirred at rt for 12 h. Next, saturated aqueous Na_2CO_3 was added. The reaction mixture was extracted with EtOAc, dried over anhydrous $MgSO_4$, filtered, and concentrated. The crude product was purified by silica gel chromatography (0−25% EtOAc in CH_2Cl_2) to give **9b** (48% yield) as a yellow solid.

N-(3-Methoxyphenyl)-[1]benzopyrano[4,3-c]pyrazol-4(2H)-one (9c). Intermediate **6a** (2.1 mmol, prepared from **5a** following the procedure described above) was dissolved in 3 mL of EtOH then was added to **9b** (2.1 mmol) suspended in 3 mL of EtOH. To this mixture was added DIPEA (8.4 mmol). The reaction mixture was stirred at rt for 12 h and then evaporated in vacuo. The crude product was partitioned between aqueous NH_4Cl and EtOAc. The organic layer was dried over anhydrous $MgSO_4$, filtered, and concentrated. The material was purified by silica gel chromatography using 0−20% EtOAc in CH_2Cl_2 as eluent to give **9c** as a white solid (56% yield).

General Procedure for 11a−c. Compounds **7a** or **10a−b** (8.6 mmol) were suspended in 15 mL of EtOH with ethyl hydrazinoacetate hydrochloride (9.5 mmol). Acetic acid (30 μL) was added. The mixture was refluxed at 105 °C for 30 min (for **11a**) or 2 h (for **11b−c**) and then allowed to cool to rt. The reaction mixture was evaporated in vacuo, partitioned between aqueous $NaHCO_3$ and EtOAc. The organic layer was dried over anhydrous $MgSO_4$, filtered, and concentrated. The crude product was purified by silica gel

chromatography using 20−75% EtOAc in hexane as eluent to give products **11a**−**c**.

[1]Benzopyrano[4,3-c]pyrazole-1(4H)acetic Acid (12a). Compound **11a** (7.3 mmol) was dissolved in 30 mL of THF, and then 18 mL of aqueous LiOH (2M) was added. The mixture was stirred at rt for 12 h, and then 5% aqueous HCl was added until the pH = 2. The mixture was evaporated to dryness, and then the residue was dissolved in EtOAc, concentrated to dryness, and used without further purification. The intermediate was dissolved in 8 mL of DMF, and then 3.6 mL of TEA and 1.23 g of EDC were added in order to reform the lactone. The mixture was stirred at rt for 18 h, and then 5% aqueous HCl was added until the pH = 2. The mixture was evaporated in vacuo, partitioned between EtOAc and aqueous NH4Cl. The organic layer was evaporated in vacuo to give **12a**, which was used without further purification (75% yield).

General Procedure for 12b−c. Compound **11b**−**c** (4.6 mmol) was dissolved in 15 mL of THF, and 9 mL of aqueous LiOH (2M) was added. The mixture was stirred at rt for 12 h, then 5% aqueous HCl was added until pH = 2. The mixture was evaporated in vacuo. The material was partitioned between EtOAc and H_2O. The organic layer was evaporated and **12b**−**c** used without further purification.

General Procedure for 13a−f. Acids **12a**−**c** (1.3 mmol), anilines (1.2 mmol), and DIPEA (5.2 mmol) were dissolved in 6 mL of DMF. To this solution was added HBTU (1.3 mmol). The mixture was stirred at rt for 12 h. Aqueous NH_4Cl (20 mL) was added and mixture extracted with EtOAc (20 mL × 3). The organic extracts were combined, dried over anhydrous $MgSO_4$, filtered, and concentrated to give material that was purified by silica gel chromatography using 0−100% EtOAc in hexane as eluent or recrystallization in 70% EtOAc in hexane to give **13a**−**f**.

ASSOCIATED CONTENT

Ⓢ Supporting Information

Procedures for **2l**, **7b**, and **10a**−**b**, compound characterization, IC_{50} determinations, gene cloning, protein expression, crystallization, and statistics for data collection/refinement of the X-ray crystal structure. This material is available free of charge via the Internet at http://pubs.acs.org.

Accession Codes
PDB ID code: 4QJ1.

AUTHOR INFORMATION

Corresponding Author
*Phone: 1-713-743-1274. E-mail: gdcuny@central.uh.edu.

Notes
The authors declare no competing financial interest.

ACKNOWLEDGMENTS

ABBREVIATIONS USED

Cp, *Cryptosporidium parvum*; DIPEA, *N,N*-diisopropylethylamine; IMP, inosine 5′-monophosphate; IMPDH, IMP dehydrogenase; ND, not determined; HBTU, *N,N,N,N*-tetramethyl-*O*-(1*H*-benzotriazol-1-yl)uronium hexafluorophosphate; EDC, 1-ethyl-3-(3-dimethylamino-propyl)carbodiimide; rt, room temperature; TEA, triethylamine; TFA, trifluoroacetic acid; XMP, xanthosine 5′-monophosphate

REFERENCES

(1) (a) Striepen, B. Parasitic infections: time to tackle cryptosporidiosis. *Nature* **2013**, *503*, 189−191. (b) Guerrant, R. L.; Oria, R. B.; Moore, S. R.; Oria, M. O.; Lima, A. A. Malnutrition as an enteric infectious disease with long-term effects on child development. *Nutr. Rev.* **2008**, *66*, 487−505.

(2) Fayer, R. *Cryptosporidium*: a water-borne zoonotic parasite. *Vet. Parasitol.* **2004**, *126*, 37−56.

(3) DuPont, H. L.; Chappell, C. L.; Sterling, C. R.; Okhuysen, P. C.; Rose, J. B.; Jakubowski, W. The infectivity of *Cryptosporidium parvum* in healthy volunteers. *N. Engl. J. Med.* **1995**, *332*, 855−859.

(4) Mead, J. R. Cryptosporidiosis and the challenges of chemotherapy. *Drug Resist. Updates* **2002**, *5*, 47−57.

(5) Hedstrom, L. IMP dehydrogenase: structure, mechanism, and inhibition. *Chem. Rev.* **2009**, *109*, 2903−2928.

(6) Striepen, B.; Pruijssers, A. J.; Huang, J.; Li, C.; Gubbels, M. J.; Umejiego, N. N.; Hedstrom, L.; Kissinger, J. C. Gene transfer in the evolution of parasite nucleotide biosynthesis. *Proc. Natl. Acad. Sci. U. S. A.* **2004**, *101*, 3154−3159.

(7) Xu, P.; Widmer, G.; Wang, Y.; Ozaki, L. S.; Alves, J. M.; Serrano, M. G.; Puiu, D.; Manque, P.; Akiyoshi, D.; Mackey, A. J.; Pearson, W. R.; Dear, P. H.; Bankier, A. T.; Peterson, D. L.; Abrahamsen, M. S.; Kapur, V.; Tzipori, S.; Buck, G. A. The genome of *Cryptosporidium hominis*. *Nature* **2004**, *431*, 1107−1112.

(8) Abrahamsen, M. S.; Templeton, T. J.; Enomoto, S.; Abrahante, J. E.; Zhu, G.; Lancto, C. A.; Deng, M.; Liu, C.; Widmer, G.; Tzipori, S.; Buck, G. A.; Xu, P.; Bankier, A. T.; Dear, P. H.; Konfortov, B. A.; Spriggs, H. F.; Iyer, L.; Anantharaman, V.; Aravind, L.; Kapur, V. Complete genome sequence of the apicomplexan *Cryptosporidium parvum*. *Science* **2004**, *304*, 441−445.

(9) Striepen, B.; White, M. W.; Li, C.; Guerini, M. N.; Malik, S. B.; Logsdon, J. M., Jr.; Liu, C.; Abrahamsen, M. S. Genetic complementation in apicomplexan parasites. *Proc. Natl. Acad. Sci. U. S. A.* **2002**, *99*, 6304−6309.

(10) Allison, A. C.; Kowalski, W. J.; Muller, C. D.; Eugui, E. M. Mechanisms of action of mycophenolic acid. *Ann. N. Y. Acad. Sci.* **1993**, *696*, 63−87.

(11) Allison, A. C.; Eugui, E. M. Mycophenolate mofetil and its mechanisms of action. *Immunopharmacology* **2000**, *47*, 85−118.

(12) Umejiego, N. N.; Gollapalli, D.; Sharling, L.; Volftsun, A.; Lu, J.; Benjamin, N. N.; Stroupe, A. H.; Riera, T. V.; Striepen, B.; Hedstrom, L. Targeting a prokaryotic protein in a eukaryotic pathogen: identification of lead compounds against cryptosporidiosis. *Chem. Biol.* **2008**, *15*, 70−77.

(13) Hedstrom, L.; Liechti, G.; Goldberg, J. B.; Gollapalli, D. R. The antibiotic potential of prokaryotic IMP dehydrogenase inhibitors. *Curr. Med. Chem.* **2011**, *18*, 1909−1918.

(14) Mandapati, K.; Gorla, S. K.; House, A. L.; McKenney, E. S.; Zhang, M.; Rao, S. N.; Gollapalli, D. R.; Mann, B. J.; Goldberg, J. B.; Cuny, G. D.; Glomski, I. J.; Hedstrom, L. Repurposing *Cryptosporidium* inosine 5′-monophosphate dehydrogenase inhibitors as potential antibacterial agents. *ACS. Med. Chem. Lett.* **2014**, *5*, 846−850.

(15) Gorla, S. K.; Kavitha, M.; Zhang, M.; Chin, J. E.; Liu, X.; Striepen, B.; Makowska-Grzyska, M.; Kim, Y.; Joachimiak, A.; Hedstrom, L.; Cuny, G. D. Optimization of benzoxazole-based inhibitors of *Cryptosporidium parvum* inosine 5′-mono phosphate dehydrogenase. *J. Med. Chem.* **2013**, *56*, 4028−4043.

(16) Gorla, S. K.; Kavitha, M.; Zhang, M.; Liu, X.; Sharling, L.; Gollapalli, D. R.; Striepen, B.; Hedstrom, L.; Cuny, G. D. Selective and potent urea inhibitors of *Cryptosporidium parvum* inosine 5′-monophosphate dehydrogenase. *J. Med. Chem.* **2012**, *55*, 7759−7771.

(17) Johnson, C. R.; Gorla, S. K.; Kavitha, M.; Zhang, M.; Liu, X.; Striepen, B.; Mead, J. R.; Cuny, G. D.; Hedstrom, L. Phthalazinone

inhibitors of inosine-5′-monophosphate dehydrogenase from *Cryptosporidium parvum*. *Bioorg. Med. Chem. Lett.* **2013**, *23*, 1004−1007.

(18) Kirubakaran, S.; Gorla, S. K.; Sharling, L.; Zhang, M.; Liu, X.; Ray, S. S.; Macpherson, I. S.; Striepen, B.; Hedstrom, L.; Cuny, G. D. Structure−activity relationship study of selective benzimidazole-based inhibitors of *Cryptosporidium parvum* IMPDH. *Bioorg. Med. Chem. Lett.* **2012**, *22*, 1985−1988.

(19) Gorla, S. K.; McNair, N. N.; Yang, G.; Gao, S.; Hu, M.; Jala, V. R.; Haribabu, B.; Striepen, B.; Cuny, G. D.; Mead, J. R.; Hedstrom, L. Validation of IMP dehydrogenase inhibitors in a mouse model of cryptosporidiosis. *Antimicrob. Agents Chemother.* **2014**, *58*, 1603−1614.

(20) Leleti, M. R.; Pennell, A. M. K.; Thomas, W. D.; Zhang, P. CXCR4 modulators. WO2007115231, 2007.

(21) Sosnovskikh, V. Y.; Moshkin, V. S.; Kodess, M. I. On the reaction of 3-cyanochromones with phenyl- and methylhydrazines: Structural revision and a simple synthesis of chromeno[4,3-*c*]pyrazol-4-ones. *J. Heterocycl. Chem.* **2010**, *47*, 629−633.

(22) Farazi, T.; Leichman, J.; Harris, T.; Cahoon, M.; Hedstrom, L. Isolation and characterization of mycophenolic acid-resistant mutants of inosine-5′-monophosphate dehydrogenase. *J. Biol. Chem.* **1997**, *272*, 961−965.

(23) Mortimer, S. E.; Hedstrom, L. Autosomal dominant retinitis pigmentosa mutations in inosine 5′-monophosphate dehydrogenase type I disrupt nucleic acid binding. *Biochem. J.* **2005**, *390*, 41−47.

(24) Umejiego, N. N.; Li, C.; Riera, T.; Hedstrom, L.; Striepen, B. *Cryptosporidium parvum* IMP dehydrogenase: identification of functional, structural, and dynamic properties that can be exploited for drug design. *J. Biol. Chem.* **2004**, *279*, 40320−40327.

(25) MacPherson, I. S.; Kirubakaran, S.; Gorla, S. K.; Riera, T. V.; D'Aquino, J. A.; Zhang, M.; Cuny, G. D.; Hedstrom, L. The structural basis of *Cryptosporidium*-specific IMP dehydrogenase inhibitor selectivity. *J. Am. Chem. Soc.* **2010**, *132*, 1230−1231.

(26) Allen, F. H.; Baalham, C. A.; Lommerse, J. P. M.; Raithby, P. R. Carbonyl−carbonyl interactions can be competitive with hydrogen bonds. *Acta Crystallogr., Sect. B: Struct. Sci.* **1998**, *B54*, 320−329.